Optics and Spectroscopy, 2025, Vol. 133, No. 1

12

# Accuracy and applicability of the standardized methods of processing the temperature data in laser and piezoelectric laser calorimetry

© K.V. Zotov[1], A.Yu. Ostapiv[1], N.V. Tereshchenko[1], O.A. Ryabushkin[2]

[1] Moscow Institute of Physics and Technology,
Dolgoprudny, Moscow Region, Russia
[2] Kotelnikov Institute of Radio Engineering and Electronics of the of the Russian Academy of Sciences,
Fryazino, Moscow region, Russia

e-mail: kirill.zotov@phystech.su ostapiv.ayu@phystech.su nikita.tereshchenko@phystech.su roa228@mail.ru

*Received October 03, 2024*
*Revised November 14, 2024*
*Accepted November 14, 2024*

Analytical expressions for the correction factors allowing to account for the finite thermal conductivity in the measuring optical absorption coeffcieint by laser calorimetry (LC) and piezoelectric resonance laser calorimetry (PRLC) methods were obtained. It was proven that the PRLC method compared to the LC method is far more resistant to the effects of the finite thermal conductivity of the sample. In practice, the main sources of error in measuring the absorption coefficient by the PRLC method turn out to be variations of the ambient temperature and of the heat transfer conditions. Modifications of the standardized methods are proposed that allows to partially account for the non-ideal experimental conditions. The correction factors that were obtained may broaden the scope of the PRLC and LC methods to the large samples or to the ones having the low heat conductivity.

**Keywords:** optical absorption, laser calorimetry, heat equation, piezoelectric laser calorimerty, piezoelectric resonance.

DOI: 10.61011/EOS.2025.01.60569.7073-24

## Introduction

Currently, laser calorimetry (LC) is a standardized method for measuring optical absorption coefficients [1]. This technique measures the temperature dependence of the sample on time $T(t)$ when heated by laser radiation during time $t_0$ and subsequent cooling after switching off the laser source. To determine the optical absorption coefficient, several methods have been proposed, called exponential, pulse, and gradient [2]. Each of them is based on a heat balance equation that does not take into account the temperature distribution inside the sample:

$$\begin{cases} \frac{\partial T}{\partial t} = \bar{Q}\theta(t_0 - t) - \Gamma(T - T_a) \\ T(0) = T_a, \end{cases} \tag{1}$$

where $\bar{Q} = P(1 - \exp(\alpha L))/mc \approx \alpha LP/mc$ — sample-averaged heat source associated with laser radiation absorption under low optical absorption $\alpha L \ll 1$, $P$ — radiation power, $L$ — sample length, $\theta(t)$ — Heaviside theta-function, $t_0$ — moment of deactivation of laser radiation, $m = \rho V$ — weight of sample, $\rho$ — density, $V$ — volume, $c$ — specific heat capacity, $\alpha$ — optical absorption coefficient, $\Gamma = hS/mc$ — rate of heat exchange, $h$ — heat-exchange coefficient, $S$ — sample surface area, $T_a$ — environmental temperature.

The gradient method analyzes the difference in temperature derivatives at time points corresponding to the same temperature $T_0$ during heating and cooling:

$$G = \left(\frac{\partial T}{\partial t}\right)\Big|_{t=t_0}^{t<t_0} - \left(\frac{\partial T}{\partial t}\right)\Big|_{T=T_0}^{t>t_0}. \tag{2}$$

From (1) it follows, that under unchanged environmental temperature $G \equiv \bar{Q}$.

Assuming the constancy of the parameters $\Gamma$ and $T_a$, the solution of equation (1) is expressed as

$$T(t) = T_a + \frac{\bar{Q}}{\Gamma}\begin{cases} 1 - e^{-\Gamma t}, & t \leq t_0 \\ e^{-\Gamma t}\left(e^{\Gamma t_0} - 1\right), & t > t_0 \end{cases} \tag{3}$$

Exponential and pulse methods are based on the approximation of the experimental dependence $T(t)$ by an exponential function

$$f(t) = A + Be^{-Ct} \tag{4}$$

during heating $(t < t_0)$ and cooling $(t > t_0)$ respectively. The set of optimal parameters $A$, $B$ and $C$ gives a possibility to define the heat source $\bar{Q}$. Next, we will denote the values obtained by approximating the kinetics of heating by index exp, and the kinetics of cooling —by index "puls". In case of exponential method:

$$E = A_{\exp}C_{\exp} = \bar{Q}, \tag{5}$$

for the pulse method:

$$I = \frac{C_{\text{puls}} f(t_0/2)}{2\text{sh}(C_{\text{puls}} t_0/2)} = \bar{Q}. \tag{6}$$

The final thermal conductivity of the sample distorts the results of all the above-mentioned techniques, but the gradient method is the most sensitive [3], because the value $G$ is strongly dependent on the position of the external temperature sensor. For this reason, the gradient method was excluded from ISO 11551 standard in 2003. Despite this, it is the only one that allows measuring the time dependence of the optical absorption coefficient, which opens up wide possibilities for studying the optical elements degradation under the influence of laser radiation [4].

One of the main disadvantages of laser calorimetry is the use of an external thermal sensor, the temperature of which cannot be fully identified with the temperature of the sample due to the presence of thermal resistance between the sample and the sensor. Moreover, the thermal sensor may absorb scattered radiation which result is distortion of readings [2]. For samples with piezoelectric properties (in particular, all nonlinear optical crystals have such properties), a piezo-resonance laser calorimetry (PRLC) technique has been developed where temperature dependence of the frequencies of the sample's intrinsic acoustic modes is used. After pre-calibration, the frequency change during the heating process can be converted into a temperature change. Since the acoustic mode is distributed over the sample, the temperature measured in this way can be identified with the average crystal temperature [5].

The purpose of this study was a theoretical analysis of the basic assumptions used in standardized methods of processing temperature kinetics, and an assessment of their effect on the measured value of the optical absorption coefficient, as well as an experimental verification of the applicability of these methods for PRLC.

## Consideration of the final thermal conductivity of the sample

To account for the sample's final thermal conductivity, it is necessary to switch from the equation of thermal balance to the equation of thermal conductivity. We will assume that the crystal temperature is measured relative to the environment, which is constant over time. Then, in the most general form, the equation of thermal conductivity for a region with boundary conditions as Newton–Richmann law at the boundary of the region and with initial conditions corresponding to the thermal equilibrium of the sample with the environment, it will be written as follows:

$$\begin{cases} \frac{\partial T(\mathbf{r},\mathbf{t})}{\partial t} = a\Delta T(\mathbf{r},t) + Q(\mathbf{r},t) \\ (-\kappa\nabla T(\mathbf{r},t),\mathbf{n})|_{\partial\Omega} = hT(\mathbf{r},t)|_{\partial\Omega} \\ T(\mathbf{r},0) = 0 \end{cases} \tag{7}$$

where $a = \kappa/c\rho$ — thermal diffusivity coefficient, $\kappa$ — thermal conductivity coefficient, $Q(\mathbf{r},t)$ — heat source function, $\mathbf{n}$ — external normal to the region boundary.

The standard method for solving such equations is the Fourier method. The solution is found as a series with separated variables:

$$T(\mathbf{r},t) = \sum_k \tau_k(t)s_k(\mathbf{r}). \tag{8}$$

The functions $s_k(\mathbf{r})$ are eigen functions for the Laplace operator satisfying the boundary conditions:

$$\begin{cases} \Delta s_k(\mathbf{r}) = -\lambda_k s_k(\mathbf{r}) \\ (-\kappa\nabla s_k(\mathbf{r}),\mathbf{n})|_{\partial\Omega} = hs_k(\mathbf{r})|_{\partial\Omega} \end{cases} \tag{9}$$

When considering the boundary conditions it naturally results in determining the Biot number, which characterizes the uniformity of the temperature distribution $b = hR/\kappa$, where $R$ is the characteristic sample size.

It is known that the system of functions $s_k(r)$ is complete and orthogonal in the space $L_2(\Omega)$ of square integrable functions on $\Omega$ [7], therefore, the expansion is true and, in addition, we can write:

$$Q(\mathbf{r},t) = \sum_k q_k(t)s_k(\mathbf{r}) \tag{10}$$

where coefficients $q_k$:

$$q_k(t) = \frac{(Q,s_k)}{\| s_k \|^2} = \frac{\int\limits_\Omega Q(\mathbf{r},t)s_k(\mathbf{r})d\Omega}{\int\limits_\Omega s_k^2(\mathbf{r})d\Omega}. \tag{11}$$

By substituting (8) and (11) into (7) we obtain equations for determining the coefficients $\tau_k$:

$$\begin{cases} \frac{d\tau_k(t)}{dt} = q_k(t) - a\lambda_k\tau_k(t) \\ \tau_k(0) = 0 \end{cases} \tag{12}$$

Then, the solution of equation (12) in case of $q_k(t) = q_k\theta(t_0 - t)$ is expressed as

$$\tau_k(t) = \frac{q_k}{a\lambda_k}\begin{cases} 1 - e^{a\lambda_k t}, & t \le t_0 \\ e^{-a\lambda_k t}(e^{a\lambda_k t_0} - 1), & t > t_0 \end{cases} \tag{13}$$

Thus, the time dependence of each decomposition term is similar to solving the heat balance equation, with the characteristic time $1/a\lambda_k$ and the value $q_k$ as the heat source. In most practically significant cases, the characteristic time for harmonics with numbers $k > 1$ is negligible compared to the measurement time, and their contribution to temperature kinetics is reduced to a constant:

$$T(\mathbf{r},t) = \tau_1(t)s_1(\mathbf{r}) + \sum_{k=1}^{+\infty} \frac{q_k}{a\lambda_k}s_k(\mathbf{r})\theta(t_0 - t). \tag{14}$$

The average temperature measured in the piezo-resonance laser calorimetry method is expressed in terms of averaged functions $\bar{s_k}(\mathbf{r})$. Integrating both parts of the upper equality in (9) over $\Omega$ domain and applying Ostrogradsky–Gauss theorem, we obtain the expression $\bar{s_k}(\mathbf{r})$ through the values of the function $s_k$ at the boundary of the domain:

$$\bar{s_k}(\mathbf{r}) = \frac{h}{\kappa\lambda_k|\Omega|}\int\limits_{\partial\Omega} s_k dS, \tag{15}$$

where $|\Omega|$ — $d$-dimension volume of $\Omega$ domain.

In approximation (14), the exponential temperature-time dependence is determined by the first term of the expansion, hence from (13), $C_{\text{exp}} = C_{\text{puls}} = a\lambda_1$. The value $A_{\text{exp}}$ represents itself a maximal heating at $t \to \infty$, which is a series of terms $q_k/a\lambda_k$. Then we can write:

$$E(\mathbf{r})a\lambda_1 \sum_k \frac{q_k}{a\lambda_k} s_k(\mathbf{r}) = q_1 s_1(\mathbf{r})$$

$$+\lambda_1 \sum_{k=2}^{+\infty} \frac{q_k}{\lambda_k} s_k(\mathbf{r}) = q_1 s_1(\mathbf{r}) + \delta(\mathbf{r}). \tag{16}$$

For the pulse method, the solution of the optimization problem gives the following expressions for the parameters $A_{\text{puls}}$, $B_{\text{puls}}$:

$$A_{\text{puls}} = 0,$$

$$B_{\text{puls}} = 2e^{a\lambda_1 t_0/2}\text{sh}(a\lambda_1 t_0/2)\frac{q_1}{a\lambda_1}s_1(\mathbf{r})$$

$$+\frac{\lambda_1}{2a}\frac{\exp(a\lambda_1(t_0+\Delta t_c/2))}{\text{sh}(a\lambda_1\Delta t_c/2)}\sum_{k=2}^{\infty}\frac{q_k}{\lambda_k^2}s_k(\mathbf{r}), \tag{17}$$

where $\Delta t_c$ — cooling down time. Substituting results in the expression:

$$I(\mathbf{r}) = q_1 s_1(\mathbf{r}) + \frac{\exp(a\lambda_1(t_0+\Delta t_c/2))}{2\text{sh}(a\lambda_1 t_0/2)\text{sh}(a\lambda_1\Delta t_c/2)}$$

$$\times\lambda_1^2\sum_{k=2}^{\infty}\frac{q_k}{\lambda_k^2}s_k(\mathbf{r}) = q_1 s_1(\mathbf{r}) + \delta_{\text{puls}}(\mathbf{r}). \tag{18}$$

In the case of the gradient method, assuming that the difference in temperature derivatives is taken at the time points at which (14) is performed, we obtain from (7) and (13):

$$G(\mathbf{r}) = q_1 s_1(\mathbf{r})\left[e^{-a\lambda_1 t_h} + e^{-a\lambda_1 t_c}\left(e^{a\lambda_1 t_0} - 1\right)\right], \tag{19}$$

where the moments of time $t_h$ and $t_c$ are defined based on condition of temperatures equality: $T(\mathbf{r}, t_n) = T(\mathbf{r}, t_c)$, $t_h \leq t_0$, $t_c \geq t_0$. By substituting (13) and (14), we obtain the ratio

$$e^{-a\lambda_1 t_h}+e^{-a\lambda_1 t_c}\left(e^{-a\lambda_1 t_0}-1\right) = 1+\frac{\lambda_1}{q_1 s_1(\mathbf{r})}\sum_{k=2}^{+\infty}\frac{q_k}{\lambda_k}s_k(\mathbf{r}). \tag{20}$$

**Table 1.** Model parameters

| | |
|---|---|
| Specific heat capacity c [9] | 1060 J/kg/K |
| Density $\rho$ [9] | 2747 kg/m$^3$ |
| Thermal conductivity coefficient $\kappa$ [9] | 3.5 W/m/K |
| Beam radius over level $1/e^2$ $w$ | 1 mm |
| Dimensions $W \times H \times L$ | $1 \times 1 \times 5$ cm$^3$ |

Substitution of (20) into (19) gives

$$G(\mathbf{r}) = q_1 s_1(\mathbf{r}) + \lambda_1\sum_{k=2}^{+\infty}\frac{q_k}{\lambda_k}s_k(\mathbf{r}) = q_1 s_1(\mathbf{r}) + \delta(\mathbf{r}). \tag{21}$$

From expressions (16), (18), (21) It follows that for all three methods, the first term of the expansion is determined with some additive correction reflecting the influence of the higher terms of the expansion. For the exponential and gradient methods this correction is equal:

$$\delta(\mathbf{r}) = \lambda_1\sum_{k=2}^{+\infty}\frac{q_k}{\lambda_k}s_k(\mathbf{r}), \tag{22}$$

for the pulse method:

$$\delta_{\text{plus}}(\mathbf{r}) = \frac{\exp(a\lambda_1(t_0+\Delta t_c/2))}{2\text{sh}(a\lambda_1 t_0/2)\text{sh}(a\lambda_1\Delta t/2)}\lambda_1^2\sum_{k=2}^{\infty}\frac{q_k}{\lambda_k^2}s_k(\mathbf{r}). \tag{23}$$

The terms of the series (22) and (23) decrease rapidly with increasing numbers, and the correction for the pulse method is smaller due to the dependence $1/\lambda_k^2$ instead of $1/\lambda_k$. The transition to PRLC method consists in averaging the eigen function $s_k(\mathbf{r})$, which increases the degree of $\lambda_k$ in appropriate terms by one (see (15)).

If the temperature has a slightly inhomogeneous distribution ($b \ll 1$) the eigen function $s_1(r)$ is almost close to unity, and the expression $\underline{q}_1 s_1(\mathbf{r})$ turns out to be close to the averaged heat source $\bar{Q}$. It can be written:

$$q_1 s_1(\mathbf{r}) = \gamma(\mathbf{r})\bar{Q}. \tag{24}$$

Thus, the absorption coefficient $\alpha$, determined by processing experimental data, and the true absorption coefficient $\alpha_0$ are related by the ratio:

$$\alpha(\mathbf{r}) = \gamma(\mathbf{r})\alpha_0 + \frac{mc}{PL}\delta(\mathbf{r}), \tag{25}$$

where $r$ — radius-vector of the measurement point.

## Asymptotic estimate of correction coefficients for the rectangular geometry of the sample

The specific type of eigen functions $s_k(\mathbf{r})$ depends on the geometry of the sample and the boundary conditions (heat transfer coefficient). In addition, the expansion coefficients

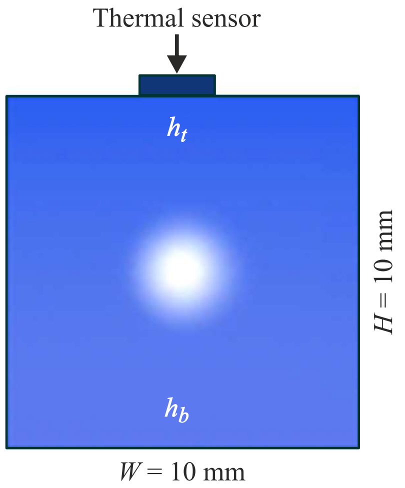

**Figure 1.** Configuration of the thermal sensor location used in the modelling. The intensity profile of the laser beam used in the experiment is shown in white to scale.

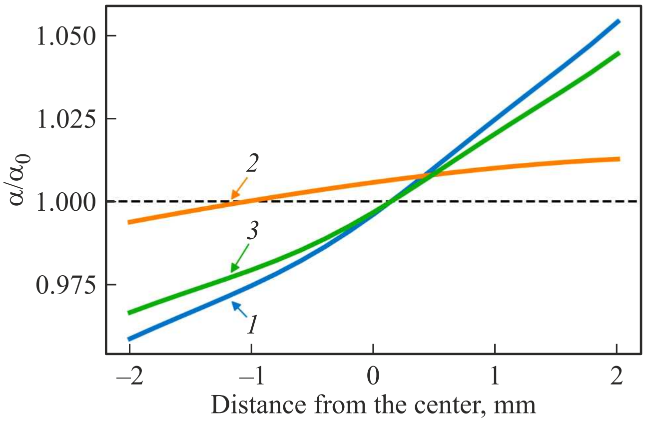

**Figure 2.** Deviation of the measured absorption coefficient in LC method versus position of the beam relative to the crystal's center. *1* — exponential method, *2* — pulse method, *3* — gradient method.

of $q_k$ vary depending on the shape of the laser beam and the place where it enters the crystal. To further specify the expressions for the correction factors $\gamma$ and $\delta$, it is necessary to set all these parameters. In particular, the correction function for the gradient method was considered in [8] for the case of a cylindrical sample heated by Gaussian laser beam passing through the center of the crystal.

However, in practice, it is impossible to guarantee the uniformity of the heat transfer coefficient $h$ on different faces of the sample, as well as to ensure the exact coincidence of the sample centers and the laser beam.

In this section, we evaluate the influence of the two aforesaid factors on the accuracy of determining the optical absorption coefficient. LBO crystal was considered within the mathematical model. The model parameters are given in Table 1.

Within the framework of the model, the temperature on the upper face of the sample for LC technique and the average temperature for PRLC technique were analyzed. The heat transfer coefficients on the upper and lower sides of the parallelepiped were assumed to be different, while their average value was set constant, since it is this value that is determined experimentally from the temperature kinetics. The beam was also shifted along Y-axis from the crystal's center (Fig. 1).

Figure 2 shows the dependence of the measured absorption coefficient for all three methods on the position of the beam when the heat transfer coefficients on the upper and lower faces of the crystal are equal. As the beam approaches the face on which the temperature is measured, the amplitude heating changes significantly. The results from the exponential method are most influenced by this. The pulse method turns out to be the most stable to beam displacement, which is consistent with the theoretical conclusion that the additive correction is small (23).

Figure 3 shows the simulation results under various conditions of heat exchange of the sample with the environment. As the heat transfer coefficient of the face on which the temperature is measured goes up, the measured absorption coefficient decreases for all methods.

Note that the graphs for the exponential and gradient methods differ from each other, despite the coincidence of the expressions for corrections (16) and (21), since the exponential method uses the entire kinetics of heating, for the initial part of which the condition is obviously not fulfilled. When the initial section of kinetics is excluded from consideration, the graphs coincide, the graph for the exponential method with the exclusion of kinetics initial section is shown in Fig. 3, bottom left.

This said, in LC method the correction coefficients should be calculated, in fact, individually for each specific experiment, which limits their applicability in practice.

In PRLC method, on the contrary, all methods of processing temperature kinetics give the same result, and, in addition, the measured absorption coefficient is weakly dependent on the above parameters. The modeling results are shown in Fig. 4.

For PRLC, the correction factor is $\delta \approx 0$, since the average values of the eigen functions rapidly decrease to zero with increasing numbers. For a coefficient $\gamma$, if PRLC measurement method is used, the following asymptotic expression can be obtained for a sample in the form of a rectangular parallelepiped with dimensions $W \times H \times L$:

$$\bar{\gamma} = 1 + \left(\frac{1}{6} - \frac{w^2}{W^2}\right) b_W + \left(\frac{1}{6} - \frac{w^2}{H^2}\right) b_H, \tag{26}$$

where $b_w = h\kappa/2W$, $b_H = h\kappa/2H$ — corresponding formal Bio numbers along axes $x$ and $y$ respectively, $w$ — beam radius to level $1/e^2$. For our model parameters we obtain $\bar{\gamma} = 1.013$. The corresponding corrections are given in Fig. 4.

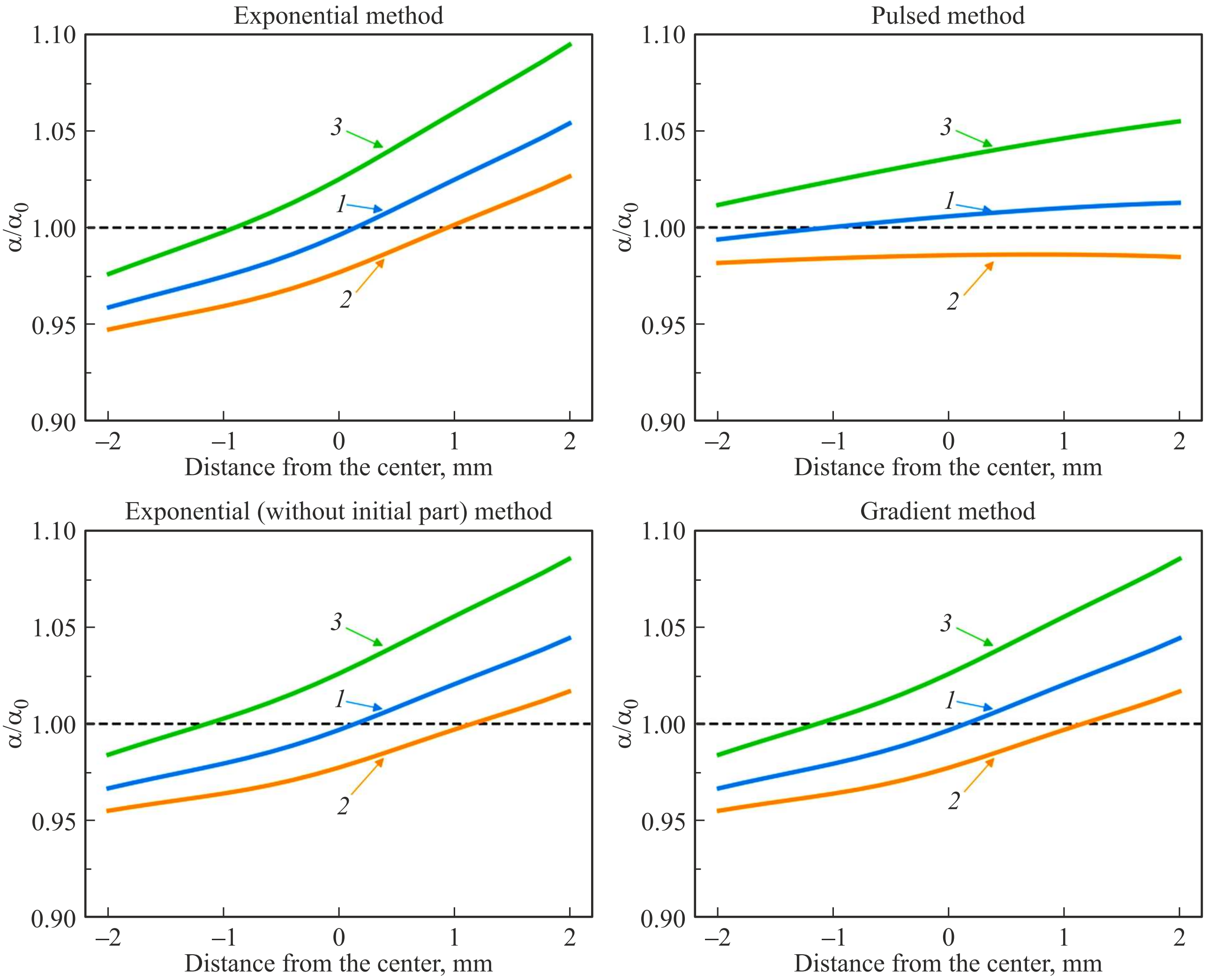

**Figure 3.** Results of modeling for LC method. Deviation of the measured absorption coefficient versus position of the beam relative to the crystal's center during heat exchange. *1* — $h_t = h_b = 30\,\mathrm{W/m^2/K}$, *2* — $h_t = 45\,\mathrm{W/m^2/K}$, $h_b = 15\,\mathrm{W/m^2/K}$, *3* — $h_t = 15\,\mathrm{W/m^2/K}$, $h_b = 45\,\mathrm{W/m^2/K}$.

## Analysis of additional sources of error in determining the optical absorption coefficient

In addition to infinite thermal conductivity of a sample, the heat balance equation (1) also implicitly relies on the assumption that the optical power of the laser, the environmental temperature and the heat transfer coefficient are not functions of time.

To assess the influence of the above factors on the error in determining the optical absorption coefficient using equation (1) with addition of additional time dependences, the model temperature kinetics were obtained. The heat balance equation (1) was solved instead of the more general equation of thermal conductivity (7), since, as shown, the resulting temperature kinetics is determined, in fact, by the first term of the expansion (8), the time dependence of which obeys an equation similar to the equation of thermal balance. Then, the deviation of the absorption coefficient recovered by various methods from the set value was estimated. The numerical error in restoring the absorption coefficient for time-independent model parameters was about 0.1%.

### Influence of environmental temperature fluctuations

The time dependence of the environmental temperature leads to an additional term in the heat source function in equation (1): $\bar{Q}\theta(t-t_0) \rightarrow \bar{Q}\theta(t-t_0) - \partial T_a/\partial t$, which can be estimated by measuring the environmental temperature using an additional thermal sensor. In case of gradient method, it is enough to add the difference of the temperature derivatives to the value $G$ . However, the exponential and pulse methods rely on a type of temperature kinetics that is no longer fully described by the function (4). The

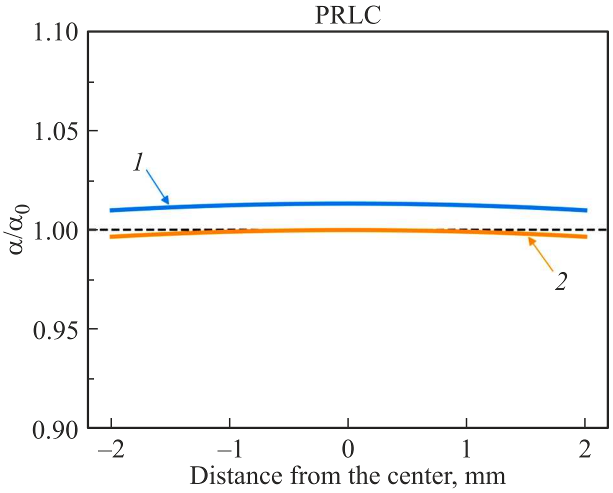

**Figure 4.** Results of modeling for PRLC method. All processing methods provide the same result. Curve *1* neglecting the correction factors *2* — with correction factors.

method of environmental temperature transformation by Fourier method allows representing it as a sum of terms $\hat{T}_a(\omega)\exp(i\omega t)$. Due to the linearity of equation (1) the resulting solution can be represented as the sum of solutions for each term of the expansion (including for $\omega = 0$, which corresponds to $T_a = \text{const}$). The addition related to the environmental temperature variation is expressed as

$$\Upsilon(t) = \sum_{\omega_k} \frac{i\omega_k \hat{T}(\omega_k)}{\Gamma + i\omega_k}[\exp(-\Gamma t) - \exp(i\omega_k t)] \qquad (27)$$

Before approximating the kinetics of temperature by an exponential function (4) it is necessary to first subtract the correction (27), which, however, requires the heat transfer rate $\Gamma$, which is itself determined from experimental kinetics - therefore an iterative correction refinement process is necessary.

Since the environmental temperature also obeys the heat balance equation, the model assumed that its kinetics had an exponential form (3) with a certain value of amplitude heating, which in our model was assumed to be equal to 30% of the crystal heating. Figure 5 shows the dependence of the modeled deviation of the measured absorption coefficient from the true value depending on the ratio of the heat transfer rates of the environment $\Gamma_a$ and the crystal $\Gamma$. As can be seen, when the ratio of these values approaches 1, the error in determining the absorption coefficient in our model exceeds 30%. The proposed procedure allows reducing the errors to almost 1%.

## The effect of the variability of the heat transfer coefficient

The heat transfer coefficient during convective heat exchange varies depending on poorly controlled parameters of the air flows flowing around the sample. This factor may be removed by placing the sample into vacuum chamber [8,10], however this approach is technically complex [11], and for LC method it makes very difficult to provide a good thermal contact with the external thermal sensor [10].

Theoretical consideration of an arbitrary time dependence of the heat transfer coefficient is complicated by considerable difficulties. In the simplest model, it can be assumed that the coefficients of heat transfer during heating and cooling have constant values that do not coincide with each other. In this case, the type of cooling kinetics depends, among other things, on the heat transfer coefficient during heating. Since the exponential method uses information obtained by approximating only the kinetics of heating, it does not require correction in this case.

In the pulse method for determination of absorption coefficient instead of $I$, defined by the formula (6), it is

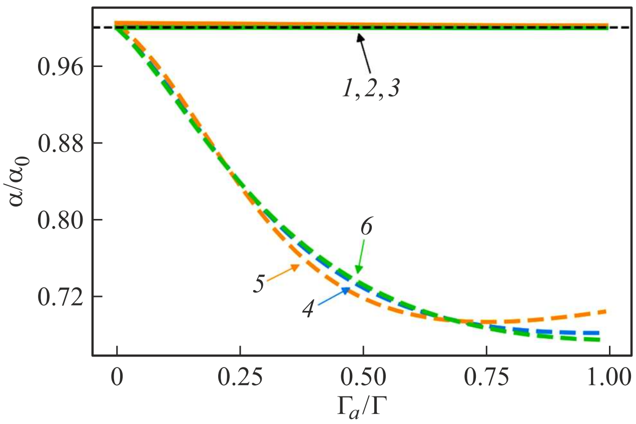

**Figure 5.** Deviation of the measured absorption coefficient versus ratio of the environment and the crystal heat transfer rates. *1, 2, 3* — exponential, pulse, and gradient methods with correction, *4, 5, 6* — exponential, pulse, and gradient methods without modifications.

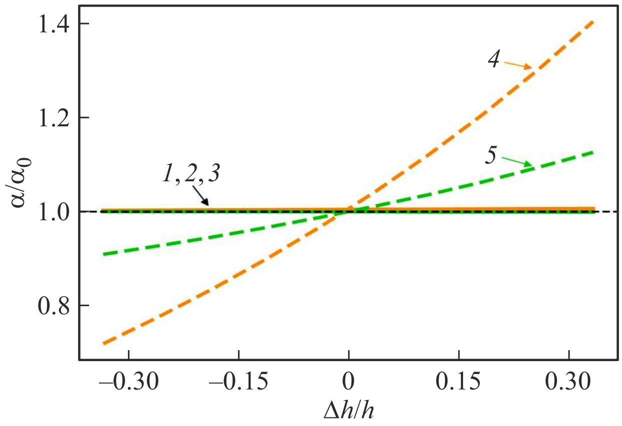

**Figure 6.** Deviation of the measured absorption coefficient versus relative changes of the heat transfer coefficient. *1* — exponential method, *2* — pulse method with correction, *3* — gradient method with correction, *4* — pulse method without modifications, *5* — gradient method without modifications.

**Table 2.** Laser source parameters

| | |
|---|---|
| Wavelength, $\lambda$ | 1030 nm |
| Pulse repetition rate | 5 MHz |
| Pulse duration | 2 ns |
| Average power $P$ | 40 W |

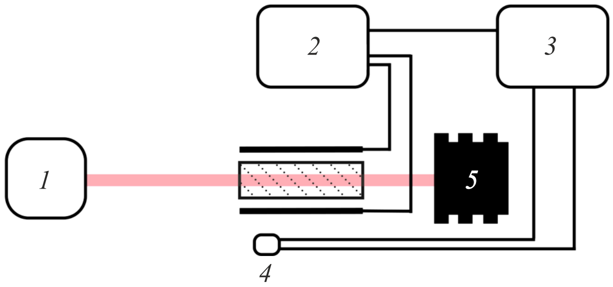

**Figure 7.** Scheme of the experimental setup. *1* — laser radiation source, *2* — crystal resonance frequency meter, *3* — computer, *4* — thermal sensor measuring the environmental temperature, *5* — power meter.

required to use $I^{\natural}$:

$$I^{\natural} = \frac{C_{\exp} f_{\text{puls}}(t_0/2)}{\exp(C_{\text{puls}} t_0/2)(1 - \exp(-C_{\exp} t_0/2))}, \tag{28}$$

At $C_{\exp} = C_{\text{puls}}$ the expression (28) transforms into (6).

In case of gradient method from defining (2) the values $G$ we obtain:

$$G = \bar{Q} - T_0(C_{\exp} - C_{\text{puls}}). \tag{29}$$

Figure 6 shows theoretical deviation of the measured absorption coefficient from the value of thermal conductivity coefficient spike relative to the average value. It was assumed that when heated, the heat transfer coefficient is equal $h - \Delta h/2$, when cooled, $h + \Delta h/2$, to keep the average value of the heat transfer coefficient constant.

## Experiment

To compare the results of processing temperature kinetics using methods described above, the absorption coefficient of the LBO crystal was measured using PRLC method. The crystal parameters coincide with those used in the model (Table 1).

A pulsed fiber ytterbium laser was used as the radiation source, the parameters of which are shown in Table 2. The sample irradiation time was 1000 s Such a long time of the experiment is associated with a large characteristic heating time of the crystal, due to its significant heat capacity. The environmental temperature was controlled by an external thermal sensor located at a distance of 10 mm from the crystal. The crystal resonance frequency was measured by method described in [12]. The experimental setup is shown in Figure 7.

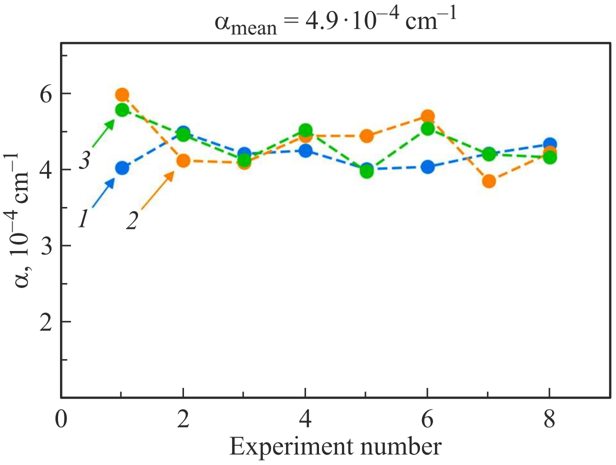

**Figure 8.** Absorption coefficient in PRLC method, determined by various methods. *1* — exponential method, *2* — pulse method, *3* — gradient method.

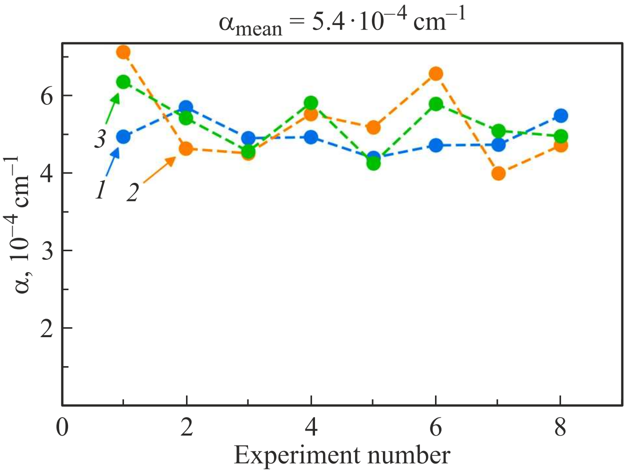

**Figure 9.** Experimental results with correction of environmental temperature changes. *1* — exponential method, *2* — pulse method, *3* —gradient method.

To estimate the random error, the experiment was repeated several times under the same conditions, each kinetics was processed using three methods.

Within one experiment, the difference in absorption coefficients determined by different methods (Fig. 8) reaches 26%. As mentioned earlier the error related to final thermal conductivity for our sample was 1%.

The measured output power instability for our laser was 2% with characteristic power change times much longer than the experimental time, which led to an error in absorption coefficient measurement of no more than 1%, according to the numerical solution of equation (1).

In our experiments, the environmental temperature showed a linear increase, followed by a linear decrease

**Table 3.** Summary table of optical absorption coefficient values in cm$^{-1}$

| Model, method | Exponential | Pulse | Gradient | Maximal difference between methods |
|---|---|---|---|---|
| Without | $4.8 \pm 0.3$ | $5.0 \pm 0.6$ | $5.0 \pm 0.4$ | 26% |
| With $\partial T_a/\partial t$ | $5.2 \pm 0.3$ | $5.5 \pm 0.8$ | $5.5 \pm 0.5$ | 30% |
| With $h$ | $5.2 \pm 0.3$ | $5.2 \pm 0.5$ | $5.3 \pm 0.5$ | 11% |

after the laser was turned off at a characteristic rate of $\sim 1 \cdot 10^{-4}$ K/s. This type of temperature-time dependence can be considered a special case of exponential dependence at $\Gamma_a \to 0$. By magnitude the added term $\partial T_a/\partial t$ was $\sim 7\%$ of this absorption-related heat source. When taking into account changes in environmental temperature in processing of experimental data (Fig. 9), the average value of the optical absorption coefficient increased by 8% for all three methods, however, within one experiment, there was still a significant (up to 30%) difference between the results obtained by different methods.

Figure 10 shows the results from formulae and for processing of experimental data modified by pulse and gradient methods. The coefficients of heat transfer during heating and cooling were determined from the approximation of the corresponding kinetic sections by an exponential function (4). Processing by exponential method didn't provide any results.

After such treatment, the spread of absorption coefficients determined by various methods decreased by almost 3 times, to 11%. Apparently, in order to completely eliminate the differences between the methods, it is necessary to develop a more complex model of the change in the heat transfer coefficient over time.

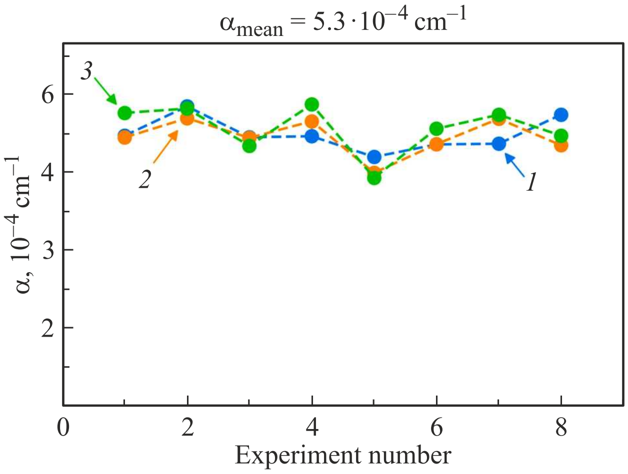

**Figure 10.** Experimental results taking into account changes in the heat transfer coefficient. *1* — exponential method, *2* — pulse method, *3* — gradient method.

The average values of the optical absorption coefficient, determined by various methods and taking into account various factors, are shown in Table 3.

## Conclusions

In piezo-resonance laser calorimetry method for determining the optical absorption coefficient, the effect of finite thermal conductivity can be taken into account using analytical corrections that depend only on the crystal parameters and its geometry. In classical LC method, the calculation of such corrections should also take into account the conditions in which the crystal is located and therefore should be carried out individually for each measurement. In PRLC method, it becomes possible to use the gradient method, which was excluded from the LC standard due to problems with measurement accuracy. This method allows measuring the optical absorption coefficient in almost real time.

Nevertheless, it has been shown that even when the heat exchange vary over time, errors in determining the optical absorption coefficient can reach much larger values. Thus, the experiment on measuring the optical absorption coefficient should be set up in such a way as to minimize the influence of these factors.

### Conflict of interest

The authors declare that they have no conflict of interest.

## References

[1] *National standard of the Russian Federation. GOST R ISO 11551-2015. Optics and optical instruments. Laser and laser-related equipment. Test method for absorptance of optical laser components* (Standartinform, Moscow 2017)

[2] U. Willamowski, T. Gross, D. Ristau, H. Welling. Proc. SPIE, **2870**, 483–494 (1996). DOI:10.1117/12.259934

[3] P. Meja, U. Broulik, U. Pfeifer, B. Steiger. Proc. SPIE, **2966**, 96–104 (1997).

[4] K.V. Zotov, N.V. Tereshchenko, A.Yu. Ostapiv, G.Yu. Ivanov, O.A. Ryabushkin. Bull. Lebedev Phys. Inst., **51** (1), S51–S57 (2024). DOI:10.3103/S1068335624600165.

[5] O.A. Ryabushkin, A.V. Konyashkin, D.V. Myasnikov, V.A. Tyrtyshnyy, O.I. Vershinin. Photonic Fiber and Crystal Devices:

Advances in Materials and Innovations in Device Applications VII, **8874**, 141–149 (2013)
DOI: 10.1117/12.2023285

[6] G.A. Aloyan, N.V. Kovalenko, I.V. Grishchenko, A.V. Konyashkin, O.A. Ryabushkin. Acoust. Phys., **68** (5), 427–434 (2022).

[7] D.S. Grebenkov, B. Nguyen. SIAM Rev., **55**(4), 601–667 (2013). DOI:10.1137/120880173

[8] G. Enrique Bernal. Appl. Opt., **14**(2), 314–321 (1975). DOI:10.1364/AO.14.000314

[9] D.N. Nikogosyan *Nonlinear optical crystals: a complete survey* (Springer Science & Business Media, 2006).

[10] R. Atkinson. Appl. Opt., **24** (4), 464–471 (1985). DOI: 10.1364/AO.24.000464

[11] U. Williamowski. *Standardisation-suited Methods for the Precise Characterisation of Absorptance, Reflectance and Transmittance of Optical Components.* PhD thesis. (Laser Zentrum Hannover e. V., Hannover, 2018).

[12] K.V. Zotov, I.V. Grischenko, A.V. Konyashkin, O.A. Ryabushkin. Appl. Opt., **62**, 4047–4051 (2023). DOI: 10.1364/AO.485644

*Translated by T.Zorina*